Cross-correlation and cross-power spectral density representation by complex spectral moments

Gioacchino Alotta[a], Mario Di Paola[a], Francesco Paolo Pinnola[a]

[a] *Dipartimento di Ingegneria Civile Ambientale, Aerospaziale, dei Materiali (DICAM), Università degli Studi di Palermo, Viale delle Scienze, Ed. 8, 90128 - Palermo, Italy*

Abstract

A new approach to provide a complete characterization of normal multivariate stochastic vector processes is presented in this paper. Such proposed method is based on the evaluation of the complex spectral moments of the processes. These quantities are strictly related to the Mellin transform and they are the generalization of the integer-order spectral moments introduced by Vanmarcke.

The knowledge of the complex spectral moments permits to obtain the power spectral densities and their cross counterpart by a complex series expansions. Moreover, with just the aid of some mathematical properties the complex fractional moments permit to obtain also the correlation and cross-correlation functions, providing a complete characterization of the multivariate stochastic vector processes.

Some numerical applications are reported in order to show the capabilities of this method. In particular, the examples regard two dimensional linear oscillators forced by Gaussian white noise, the characterization of the wind velocity field, and the stochastic response analysis of vibro-impact system under Gaussian white noise.

Keywords: Complex Spectral Moments, Mellin transform, Cross-Correlation, Cross Power Spectral Density

1. Introduction

In several structural dynamics problems the external agencies are often modeled as stochastic processes, e.g. ocean waves, earthquake excitation, wind velocity field, random vibration in mechanical devices, etc.[1, 2]. This approach to represent the real input in the structures implies that the responses of structural systems are stochastic processes too. The probabilistic characterization of such processes represents an important branch in the stochastic mechanics for the reliability analysis.

Several structural mechanical problems involve the stochastic analysis of structure under Gaussian processes. In such cases, a widespread way to get their stochastic characterization is given by two determin-

Email addresses: gioacchino.alotta@unipa.it (Gioacchino Alotta), mario.dipaola@unipa.it (Mario Di Paola), francesco.pinnola@unipa.it (Francesco Paolo Pinnola)

istic functions. That is, the auto correlation function (ACF) of the processes and/or its Fourier transform, namely the Power Spectral Density (PSD) function.

When the dynamic system is more complex and several correlated response processes are involved (e.g. multi-degree-of-freedom systems, multi-variated stochastic processes, multidimensional stochastic fields, etc.) the ACFs and the PSDs are not sufficient for a complete characterization of the processes. In fact, also the cross counterparts of ACF and PSD are needed. Moreover, the knowledge of the analytical expression of these functions are not always available for practical problems.

However, there is another way to characterize the stochastic processes that involves the Complex Spectral Moments (CSMs) [3]. This approach is based on the definition of a certain numbers of complex quantities related to a particular integral transform of the PSD function, namely Mellin transform operator[4–7]. The complex quantities obtained by the application of this integral transforms are nothing else that the generalization of the integer-order spectral moments introduced by Vanmarcke [8]. The knowledge of the CSMs provides a complete description of random processes. In fact, such complex quantities contains information in both time and frequency domain of the stochastic processes. This fact implies that they are able to reconstruct the PSD and the ACF. The capabilities of the complex moments have been shown in several articles. Precisely, they are applied for the characterization of random variables [9–11], for the digital simulation of the random processes [12, 13], for the approximated solution of the Fokker-Planck equation [14, 15], Kolmogorov-Feller equation [16], for the evaluation of the stationary correlation function of fractional-order oscillator [17], and for a new way to perform the wavelet analysis [18]. The present paper aims to extends the application of the method described in [3] in order to provide a complete characterization of stochastic response processes when the problem is multivariate stochastic vector process. In fact, it will show that CSMs are able to describe not only the PSD and ACF but also their cross-counterparts. Numerical examples are reported and contain linear and non-linear applications of the presented method.

2. Preliminary concepts

Spectral Moments (SMs) introduced by Vanamarcke [8] are integer-order moments of the one-sided power spectral density function (PSD) of the stochastic process $X(t)$. That is,

$$\lambda_X(j) = \int_0^\infty S_X(\omega)\omega^j d\omega; \qquad j = 0, 1, ... \tag{1}$$

where $S_X(\omega)$ denotes the PSD of $X(t)$. SMs give some information on the PSD, such as the variance of X ($\lambda_X(0)$) or the variance of $\dot{X}$ ($\lambda_X(2)$). However, they are not able to reconstruct the whole PSD; moreover, they do not give any information about the correlation and in many case of engineering interest they may be divergent quantities as j increase.

The generalization of spectral moments are the Complex Spectral Moments (CSMs) which definition coincide reads

$$\Lambda_X(\gamma) = \int_0^\infty S_X(\omega)\omega^\gamma d\omega; \qquad \gamma = \rho + i\eta \tag{2}$$

This definition coincides with the Mellin transform operator that is described in Appendix A. Obviously as $\gamma = 0, 1, 2, ..$ the definition in Eq. (2) coalesces with the classical SM. Mellin transform has a correspondent inverse transform that allows to construct the original function starting from the knowledge of the CSMs

$$S_X(\omega) = \frac{1}{2\pi}\int_{-\infty}^{\infty} \Lambda_X(-\gamma)\omega^{\gamma-1} d\eta; \qquad \omega > 0 \tag{3}$$

Inspection of Eq. (3) reveals that integration is performed along the imaginary axis η and ρ is fixed. Moreover, since $\Lambda_X(-\gamma) \to 0$ for $\eta \to \pm\infty$, Eq. (3) can be discretized in a summation of finite elements:

$$S_X(\omega) \simeq \frac{\Delta\eta}{2\pi}\sum_{k=-m}^{m} \Lambda_X(-\gamma_k)\omega^{\gamma_k-1}; \qquad \omega > 0 \tag{4}$$

where $\gamma_k = \rho + ik\Delta\eta$ and the truncation parameter m is such that contribution of elements with $k > m$ are negligible, therefore m defines a cut-off value $\eta_c = m\Delta\eta$ along the imaginary axis. It is worth noticing that this summation does not diverge for $\omega \to \infty$ and is able to reconstruct the function $S_X(\omega)$ in the whole interval $\omega > 0$; the value in $\omega = 0$ is excluded because divergences of the terms $\omega^{-\gamma_k}$ occur. Eqs. (3) and (4) remain valid provided ρ belongs to the so called Fundamental Strip (FS) of Mellin transform (see Appendix).

Since the PSD is a symmetric function, it can be easily reconstructed in the whole domain as:

$$S_X(\omega) = \frac{1}{2\pi}\int_{-\infty}^{\infty} \Lambda_X(-\gamma)|\omega|^{\gamma-1} d\eta \simeq \frac{\Delta\eta}{2\pi}\sum_{k=-m}^{m} \Lambda_X(-\gamma_k)|\omega|^{\gamma_k-1}; \qquad \omega \neq 0 \tag{5}$$

CSMs are useful also to represent the auto-correlation function (ACF) $R_X(\tau)$ which relationship with $S_X(\omega)$ reads as follows

$$R_X(\tau) = \int_{-\infty}^{\infty} S_X(\omega)e^{-i\omega\tau} d\omega \tag{6a}$$

$$S_X(\omega) = \frac{1}{2\pi}\int_{-\infty}^{\infty} R_X(\tau)e^{i\omega\tau} d\tau \tag{6b}$$

Eqs. (6) imply that also the ACF is a symmetric function. Application of operator Eq. (6a) to Eq. (5) yields

$$R_X(\tau) = \frac{1}{\pi}\int_{-\infty}^{\infty} \nu_c(\gamma)\Lambda_X(-\gamma)|\tau|^{-\gamma} d\eta \simeq \frac{\Delta\eta}{\pi}\sum_{k=-m}^{m} \nu_c(\gamma_k)\Lambda_X(-\gamma_k)|\tau|^{-\gamma_k}; \qquad \tau \neq 0 \tag{7}$$

where $\nu_c(\gamma_k) = \Gamma(\gamma_k)\cos(\gamma_k\pi/2)$ and $\Gamma(\cdot)$ is the Euler gamma function. More details about relationship between Eq. (5) and (7) can be found in [11]. On the other hand complex moments (CMs) of the ACF can be defined, in terms of Mellin transform, as

$$M_X(\gamma - 1) = \int_0^\infty R_X(\tau)\tau^{\gamma-1} d\tau \tag{8}$$

CMs are able to reconstruct both the ACF and the PSD as follows:

$$R_X(\tau) = \frac{1}{2\pi}\int_{-\infty}^{\infty} M_X(\gamma-1)|\tau|^{-\gamma}d\eta \simeq \frac{\Delta\eta}{2\pi}\sum_{k=-m}^{m} M_X(\gamma_k-1)|\tau|^{-\gamma_k} \tag{9a}$$

$$S_X(\omega) = \frac{1}{2\pi^2}\int_{-\infty}^{\infty} \nu_c(1-\gamma)M_X(\gamma-1)|\omega|^{\gamma-1}d\eta \simeq \frac{\Delta\eta}{2\pi^2}\sum_{k=-m}^{m} \nu_c(1-\gamma_k)M_X(\gamma_k-1)|\omega|^{\gamma_k-1} \tag{9b}$$

Comparison of Eqs. (9) with Eqs. (7) and (5) reveals that CSMs are related to CMs by simply algebraic relationship

$$M_X(\gamma_k-1) = 2\nu_c(\gamma_k)\Lambda_X(-\gamma_k) \tag{10}$$

or

$$\Lambda_X(-\gamma_k) = \frac{\nu_c(1-\gamma_k)M_X(\gamma_k-1)}{\pi} \tag{11}$$

From Eqs. (9) it is evident that a limited number of moments of complex order, say $2m+1$, is able to give information about the process both in the frequency and in time domain. This means that moments of complex order overcome some limitations of integer order moments, but in the form presented in this section it is possible to handle only univariate processes. In the next section this method is extended in order to describe also multivariate processes.

3. Characterization of multidimensional processes

When a multivariate vector process is studied, the PSD and the ACF are not enough to represent the entire vector process. The complete probabilistic is given by also cross PSD (CPSD) and/or cross correlation functions (CCF). The CPSD function $S_{X_1X_2}$ is constituted by a real even part $\hat{G}_{X_1X_2}(\omega)$ (the co-spectrum) and an imaginary odd part $\tilde{G}_{X_1X_2}(\omega)$ (the quadrature spectrum). That is,

$$S_{X_1X_2}(\omega) = \hat{G}_{X_1X_2}(\omega) + i\tilde{G}_{X_1X_2}(\omega) \tag{12}$$

where i is the imaginary unit. Relationship between CPSD and CCF is analogous to Eq. (6). However application of Eq. (6a) yields to

$$\begin{aligned} R_{X_1X_2}(\tau) = \int_{-\infty}^{\infty} S_{X_1X_2}(\omega)e^{-i\omega t}d\omega = \\ \int_{-\infty}^{\infty} \hat{G}_{X_1X_2}(\omega)\cos(\omega t)d\omega + \int_{-\infty}^{\infty} \hat{G}_{X_1X_2}(\omega)\sin(\omega t)d\omega = \\ \hat{R}_{X_1X_2}(\tau) + \tilde{R}_{X_1X_2}(\tau) \end{aligned} \tag{13}$$

being $\hat{R}_{X_1X_2}(\tau)$ and $\tilde{R}_{X_1X_2}(\tau)$ the even and odd parts of the CCF, respectively:

$$\hat{R}_{X_1X_2}(\tau) = \frac{R_{X_1X_2}(\tau) + R_{X_1X_2}(-\tau)}{2} \tag{14a}$$

$$\tilde{R}_{X_1X_2}(\tau) = \frac{R_{X_1X_2}(\tau) - R_{X_1X_2}(-\tau)}{2} \tag{14b}$$

As in the previous section, the CSMs are able to reconstruct both the real and imaginary parts of $S_{X_1X_2}(\omega)$ in the whole domain thanks to the symmetry properties of $\hat{G}_{X_1X_2}(\omega)$ and $\tilde{G}_{X_1X_2}(\omega)$. However since the CCF is not symmetric, it can be reconstructed only for $t > 0$. In order to permit the description of the whole CCF also for $t < 0$, the CSMs are defined separately for the real and imaginary part of $S_{X_1X_2}(\omega)$

$$\hat{\Lambda}_{X_1X_2}(-\gamma) = \int_0^\infty \hat{G}_{X_1X_2}(\omega)\omega^{-\gamma}d\omega \tag{15a}$$

$$\tilde{\Lambda}_{X_1X_2}(-\gamma) = \int_0^\infty \tilde{G}_{X_1X_2}(\omega)\omega^{-\gamma}d\omega \tag{15b}$$

The CPSD is easily reconstructed from the knowledge of its CSMs as

$$\begin{aligned} S_{X_1X_2}(\omega) &= \frac{1}{2\pi}\int_{-\infty}^{\infty}(\hat{\Lambda}_{X_1X_2}(-\gamma) + i\,\mathrm{sgn}(\omega)\tilde{\Lambda}_{X_1X_2}(-\gamma))|\omega|^{\gamma-1}d\eta \\ &\simeq \frac{\Delta\eta}{2\pi}\sum_{k=-m}^{m}(\hat{\Lambda}_{X_1X_2}(-\gamma_k) + i\,\mathrm{sgn}(\omega)\tilde{\Lambda}_{X_1X_2}(-\gamma_k))|\omega|^{\gamma_k-1}; \quad \omega \neq 0 \end{aligned} \tag{16}$$

Substitution of Eq. (16) in Eq. (6a) yields to

$$\begin{aligned} R_{X_1X_2}(\tau) &= \frac{1}{\pi}\int_{-\infty}^{\infty}(\nu_c(\gamma)\hat{\Lambda}_{X_1X_2}(-\gamma) + i\,\mathrm{sgn}(\tau)\nu_s(\gamma)\tilde{\Lambda}_{X_1X_2}(-\gamma))|\tau|^{-\gamma}d\eta \\ &\simeq \frac{\Delta\eta}{\pi}\sum_{k=-m}^{m}(\nu_c(\gamma_k)\hat{\Lambda}_{X_1X_2}(-\gamma_k) + i\,\mathrm{sgn}(\tau)\nu_s(\gamma_k)\tilde{\Lambda}_{X_1X_2}(-\gamma_k))|\tau|^{-\gamma_k}; \quad \tau \neq 0 \end{aligned} \tag{17}$$

where $\nu_s(\gamma_k) = \Gamma(\gamma_k)\sin(\gamma_k\pi/2)$. More details about relationship between Eq. (16) and (17) can be found in [11]. Eqs. (16) and (17) shows that CSMs are able to describe both the CPSD and the CCF; the same results is achieved by using CMs of the CCF, defined as

$$\hat{M}_{X_1X_2}(\gamma - 1) = \int_0^\infty \hat{R}_{X_1X_2}(\tau)\tau^{\gamma-1}d\tau \tag{18a}$$

$$\tilde{M}_{X_1X_2}(\gamma - 1) = \int_0^\infty \tilde{R}_{X_1X_2}(\tau)\tau^{\gamma-1}d\tau \tag{18b}$$

From the knowledge of $\hat{M}_{X_1X_2}(\gamma-1)$ and $\tilde{M}_{X_1X_2}(\gamma-1)$ both the CCF and the CPSD can be reconstructed

$$\begin{aligned} R_{X_1X_2}(\tau) &= \frac{1}{2\pi}\int_{-\infty}^{\infty}(\hat{M}_{X_1X_2}(\gamma-1) + \mathrm{sgn}(\tau)\tilde{M}_{X_1X_2}(\gamma-1))|\tau|^{-\gamma}d\eta \simeq \\ &\frac{\Delta\eta}{2\pi}\sum_{k=-m}^{m}(\hat{M}_{X_1X_2}(\gamma_k-1) + \mathrm{sgn}(\tau)\tilde{M}_{X_1X_2}(\gamma_k-1))|\tau|^{-\gamma_k}; \quad \tau \neq 0 \end{aligned} \tag{19a}$$

$$\begin{aligned} S_{X_1X_2}(\omega) &= \frac{1}{2\pi^2}\int_{-\infty}^{\infty}(\nu_c(1-\gamma)\hat{M}_{X_1X_2}(\gamma-1) + i\,\mathrm{sgn}(\tau)\nu_s(1-\gamma)\tilde{M}_{X_1X_2}(\gamma-1))|\omega|^{\gamma-1}d\eta \simeq \\ &\frac{\Delta\eta}{2\pi^2}\sum_{k=-m}^{m}(\nu_c(1-\gamma_k)\hat{M}_{X_1X_2}(\gamma_k-1) + \mathrm{sgn}(\omega)\nu_s(1-\gamma_k)\tilde{M}_{X_1X_2}(\gamma_k-1))|\omega|^{\gamma_k-1}; \quad \omega \neq 0 \end{aligned} \tag{19b}$$

Comparison of Eqs. (19) with Eqs. (16) and (17) shows that Eqs. (10) and (11) are valid for $\hat{M}_{X_1X_2}(\gamma_k - 1)$ and $\hat{\Lambda}_{X_1X_2}(-\gamma_k)$; moreover

$$\tilde{M}_{X_1X_2}(\gamma_k - 1) = 2\nu_s(\gamma_k)\tilde{\Lambda}_{X_1X_2}(-\gamma_k) \tag{20}$$

or

$$\tilde{\Lambda}_{X_1X_2}(-\gamma_k) = \frac{\nu_s(1-\gamma_k)\tilde{M}_{X_1X_2}(\gamma_k - 1)}{\pi} \tag{21}$$

CSMs or CM are then useful when the CPSD is known and the CCF is needed (or vice-versa). The relationships in Eqs. (10), (11), (20) and (21) are obtained by using the Fourier transform properties. However, they can be also demonstrated using properties of fractional operators [5, 11, 17].The knowledge of a limited number of moments guarantees that the stochastic process is entirely characterized both in frequency and in time domain also when process is multivariate stochastic vector process. It should be concluded that moments of complex order contains all the information of the stochastic process then they are an effective tool to represent stochastic processes.

4. Numerical examples

In this section some benchmark problems are presented in order to show the capability of the method.

4.1. Linear oscillators under white noise

Consider two linear oscillators driven by the same zero-mean Gaussian white noise process $W(t)$. The equations of motion of such mechanical system is

$$\begin{cases} \ddot{X}_1(t) + 2\zeta_1\omega_{01}\dot{X}_1(t) + \omega_{01}^2 X_1(t) = p_1 W(t); \\ \ddot{X}_2(t) + 2\zeta_2\omega_{02}\dot{X}_1(t) + \omega_{02}^2 X_2(t) = p_2 W(t). \end{cases} \tag{22}$$

where ζ_j $(j = 1, 2)$ is the percentage of the critical damping of the j-th oscillator, and ω_{0j} $(j = 1, 2)$ is the natural radial frequency of the j-th oscillator. For this case, both the CCF and the CPSD are known so it is possible the evaluation of CSMs by Eq.s (15) and/or the CMs by Eq.s (18). Without loss of generality, consider the PSD and CPSD, denoted $S_{X_jX_k}(\omega)$. That is,

$$S_{X_jX_k}(\tau) = \frac{p_j p_k S_0}{\left[\left(\omega_j^2 - \omega^2\right) - 2i\zeta_j\omega_j\omega\right]\left[(\omega_k^2 - \omega^2) + 2i\zeta_k\omega_k\omega\right]}, \quad j, k = 1, 2, \tag{23}$$

where the S_0 is the PSD of the white noise $W(t)$. Obviously, when $j = k$ the Eq. (23) gives the PSD functions, whereas if $j \neq k$ the CPSD functions yields. Only the CPSD and the CCF are considered below and the CSMs are used to obtain the CPSD and CCF.

The CSMs of the system are defined as

$$\hat{\Lambda}_{X_jX_k}(\tau) = \int_0^\infty \Re\left\{S_{X_jX_k}(\omega)\right\}\omega^{-\gamma}d\omega, \tag{24a}$$

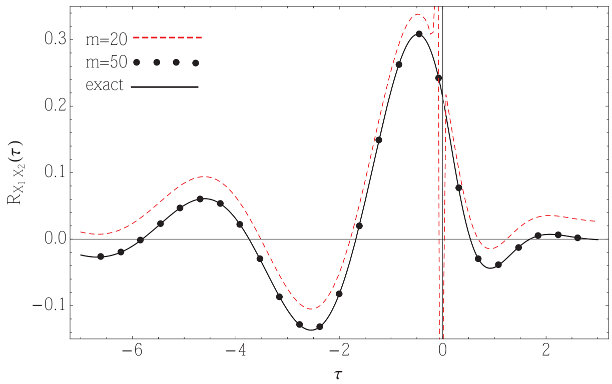

Figure 1: Exact and approximate, obtained with CSMs, cross-correlation

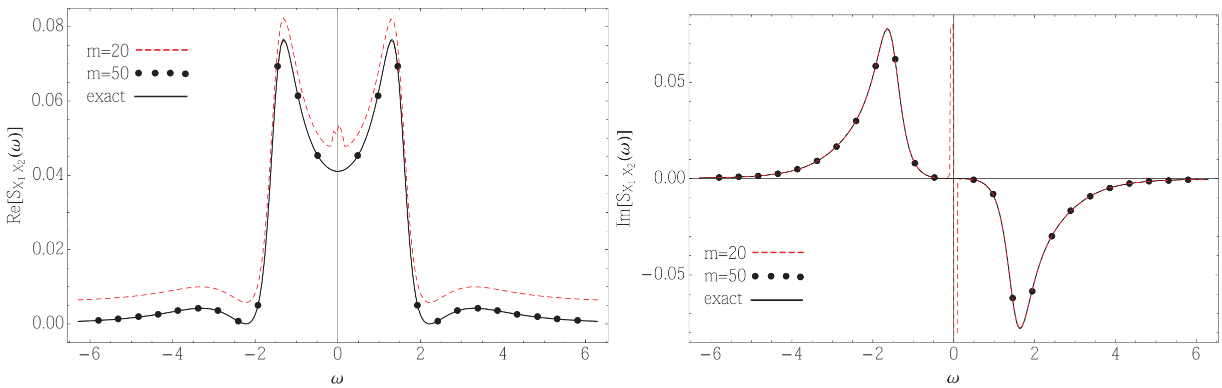

Figure 2: Exact and approximate, obtained with CSMs, CPSD

$$\tilde{\Lambda}_{X_jX_k}(\tau) = \int_0^{\infty} \Im\left\{S_{X_jX_k}(\omega)\right\}\omega^{-\gamma}d\omega, \tag{24b}$$

By the knowledge of the CSMs and with the aid of Eq. (16) the CPSD is given in another form. Moreover, by using the same CSMs and the Eq. (17) also the CCF is given. Figure 1 shows the comparison between the exact CCF and its approximated form obtained by CSMs, while the Figure 2 shows the overlap between the exact and approximate representation of real and imaginary part of CPSD, obtained by using of CSMs. For this numerical example the chosen parameters of the mechanical system are: $\omega_1 = 2\omega_2 = \pi$, $\zeta_1 = 2\zeta_2 = 1/2$, $p_1 = 4p_2 = 2$ and $S_0 = 1$. The depicted approximate representation of CCF and CPSD are performed with $\rho = 1/2$, and for different values of the number terms in the summations $m = 20$, 50, and different discretization steps $\Delta\eta = 1.5$, 0.6. It is to be noted that by appropriately selecting the number of terms in Eq. (17) the whole CCF is restored with the exception of the value in zero in which a singularity appears. Fig. 2 the CPSD is reported and compared with that obtained by Eq. (16). Therefore, for the case at hand by knowing only $2m + 1 = 51$ (complex) quantities both $R_{X_1X_2}(\tau)$ and $S_{X_1X_2}(\omega)$ may be easily reconstructed. It implies that the knowledge of a certain number of CSMs are sufficient to complete characterize the two stochastic processes $X_1(t)$ and $X_2(t)$.

4.2. Wind stochastic processes

The characterization and simulation of wind velocity fields from a probabilistic point of view have been pursued in many works [19–25]. This example shows the characterization of a two-dimensional homogeneous wind stochastic process. The velocity $\mathcal{V}(x, y, z; t)$ can be seen as a time dependent two variate-three dimensional stochastic field process, but for the sake of simplicity in this example wind speed will be characterized in a vertical plane, then the velocity field can be seen as a time dependent two variate-two dimensional stochastic field process $\mathcal{V}(y, z; t)$. The probabilistic characterization of wind velocity field is performed with the concepts reported in [20]; two cases are considered: i) in the first one the two point under consideration are located at same levels in the plane $z_1 = z_2 = h$ and, as it is shown in Eq. (26), the CPSD can be considered real; ii) in the second one it is considered two points located at different level in the same vertical line $z_1 \neq z_2$ and $y_1 = y_2$ and the CPSD is expressed as a sum of a real and an imaginary part (see Eq. (30)).

It is well known that wind speed is a stochastic process that can be decomposed into a mean value $\bar{V}(z)$ and a fluctuating part $V(y, z; t)$ as follows

$$\mathcal{V}(y, z; t) = \bar{V}(z) + V(y, z; t); \tag{25}$$

where $\bar{V}(z) = \frac{1}{k} u_* \ln(z/z_0)$ and $k = 0.4$ is the Von Karman constant, u_* is the shear velocity and z_0 is the roughness length.

Let's start with the first case, in which the CPSD is written as

$$S_{V_1V_2}(\omega) = \sqrt{S_{V_1V_1}(\omega) S_{V_2V_2}(\omega)} \exp(-f_{12}(\omega)) \tag{26}$$

where $S_{V_1V_1}(\omega) = S_{V_2V_2}(\omega) = S_{VV}(\omega)$ (because $z_1 = z_2 = h$) are the PSD of the wind velocity in the point considered

$$S_{VV}(\omega) = \frac{6.868\, \sigma_V^2 f(h) L_u(h)/h}{(\omega/2\pi)[1 + 10.302 f(h) L_u(h)/h]^{5/3}} \tag{27}$$

where $f(z) = \omega z / 2\pi \bar{V}(h)$, $L_u(z)$ is the integral length scale of turbulence, $\sigma_V^2 = \beta u^2$ is the variance of the longitudinal component of the velocity fluctuation (complete description of parameters can be found in [21]).

In Eq. (25) $\exp(-f_{12}(\omega))$ is the so called *coherency function*, in which $f_{12}(\omega)$ is given as

$$f_{12}(\omega) = \frac{|\omega| \sqrt{C_y^2 (y_1 - y_2)^2 + C_z^2 (z_1 - z_2)^2}}{2\pi[\bar{V}(z_1) + \bar{V}(z_2)]} \tag{28}$$

where C_y and C_z are appropriate decay coefficients. In this first case $z_1 = z_2 = h$, then we may write

$$f_{12}(\omega) = \frac{|\omega| C_y \eta}{4\pi \bar{V}(h)} \tag{29}$$

For this case the parameters chosen are $h = 5\,m$, $z_0 = 0.25\,m$, $C_y = 10$, $\chi = 5\,m$ and $u_* = 1\,m/sec$; the discretization parameters in the Mellin domain are $\rho = 0.5$ (see Appendix A), $\Delta\eta = 0.2$ and $m = 10$. From the CPSD we evaluated the CSMs $\Lambda_X(-\gamma)$ and with these quantities both the CPSD and the corresponding CCF have been reconstructed. In Fig. 3 approximated CPSD reconstructed with the aid of CSMs is contrasted with exact CPSD, while in Fig. 4 CCF reconstructed with CSMs is compared with CCF obtained from Monte Carlo simulations preformed with the method described in [20].

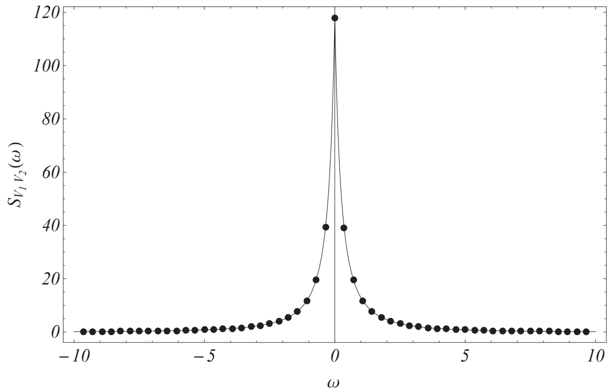

Figure 3: Exact (continuous line) and approximated (dotted line), obtained with CSMs, CPSD.

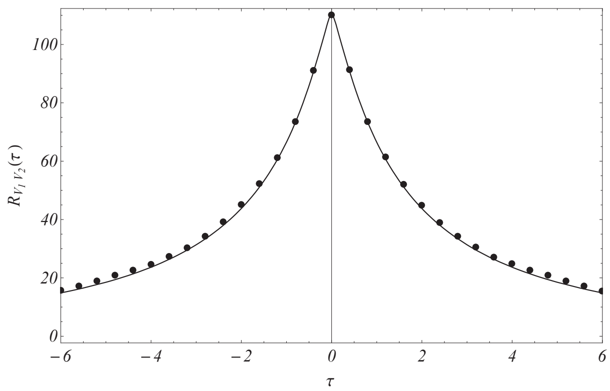

Figure 4: Cross-correlation obtained by CSMs (continuous line) vs cross-correlation obtained by Monte Carlo simulation (dotted line).

In a more realistic case the CPSD between two stochastic processes $V_1(y_1, z_1; t_1)$ and $V_2(y_2, z_2; t_2)$ is a complex function $G_{V_1V_2}(\omega)$ that can be written in the form

$$G_{V_1V_2}(\omega) = \hat{G}_{V_1V_2}(\omega) + i\tilde{G}_{V_1V_2}(\omega) \tag{30}$$

where $\hat{G}_{V_1V_2}(\omega)$ and $\tilde{G}_{V_1V_2}(\omega)$ are the so called co- and quad-spectrum, respectively. Moreover the co-spectrum is even while the quadrature one is odd.

If we consider that the two point under consideration are located in the same vertical axis (second case in this subsection) both $\hat{G}_{V_1V_2}(\omega)$ and $\tilde{G}_{V_1V_2}(\omega)$ are well established and it is possible to write

$$G_{V_1V_2}(\omega) = S_{V_1V_2}(\omega)\exp(-i\theta_{12}(\omega)) \tag{31}$$

where

$$\theta_{12}(\omega) = \frac{\omega(z_1 - z_2)}{v_{app}^{(1,2)}} \tag{32}$$

and $S_{V_1V_2}(\omega)$ has been defined in Eq. (26). For this case

$$S_{V_iV_i}(\omega) = \frac{6.868\,\sigma_V^2 f(z_i)L_u(z_i)/z_i}{(\omega/2\pi)[1 + 10.302f(z_i)L_u(z_i)/z_i]^{5/3}} \tag{33}$$

and

$$f_{12}(\omega) = \frac{|\omega|\sqrt{C_z^2(z_1 - z_2)^2}}{2\pi[\bar{V}(z_1) + \bar{V}(z_2)]} \tag{34}$$

In Eq. (32) $v_{app}^{(1,2)}$ is the apparent velocity of waves; in this example $z_0 = 0.25\,m$, $v_{app}^{(1,2)} = 15\,m/sec$, $u_* = 1\,m/sec$ and $C_z = 15$; the discretization parameters are $\rho = 0.4$ (see Appendix A), $\Delta\eta = 0.3$ and $m = 20$. In the following, Figs. 5 and 6 show the comparison between exact CPSD and its reconstruction with CSMs and between the CCF obtained with CSMs and CCF obtained with Monte Carlo simulations.

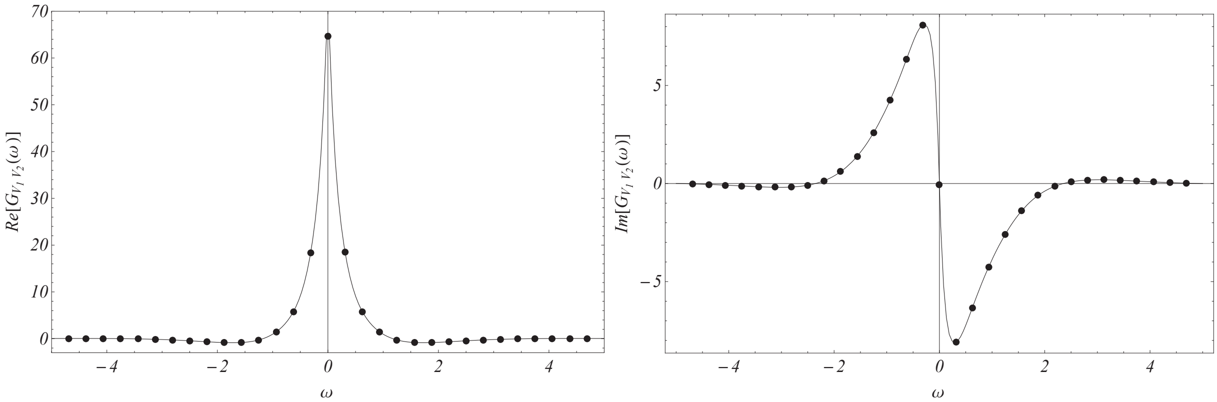

Figure 5: Exact (continuous line) and approximate (dotted line), obtained with CSMs, of real and imaginary part of CPSD.

4.3. SDOF vibro-impact system

A single degree of freedom system with a one-sided barrier forced by Gaussian white noise is considered below. Such system has been studied in terms of ACF and PSD in [26]; another approach can be found in [27]. In this section the representation of the response process is obtained by the CMs of the exact ACF of the response. It is shown that the knowledge of a certain number of such complex quantities permits to represent both ACF and PSD providing another way to describe the stochastic process. Therefore, also

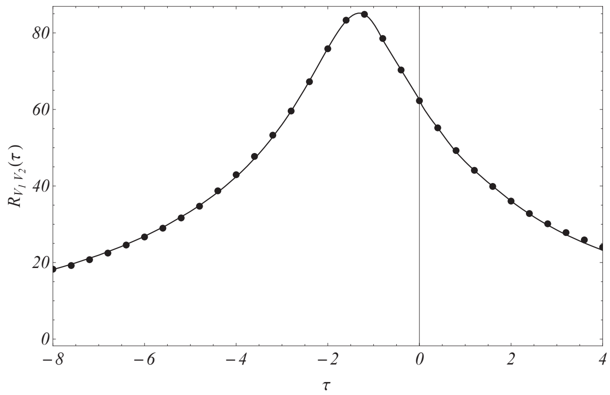

Figure 6: Cross-correlation obtained by CSMs (continuous line) vs cross-correlation obtained by Monte Carlo simulation (dotted line).

in this non-linear case the CMs are able to provide a complete characterization of the stochastic response process at hand.

Consider a vibro-impact system consisting of a SDOF system with linear spring and one-sided rigid barrier excited by a white noise force. In this way, between the impacts, the motion of such mechanical system is ruled by a linear second-order stochastic differential equation, and the impact is assumed as perfectly elastic. The case considered below is a special case in which the ACF can be found in closed form by a certain piece-wise-linear transformation of the response variable [26]. In particular, consider the equation of motion of the vibro-impact system between the impact at barrier at the position $Y = 0$,

$$\ddot{Y}(t) + 2\zeta\omega_0\dot{Y}(t) + \omega_0^2 Y(t) = W(t), \qquad Y > 0, \tag{35}$$

being $W(t)$ the zero-mean Gaussian white noise process with intensity q. The impact conditions when $Y = 0$ are

$$\dot{Y}_+(\bar{t}) = -\dot{Y}_-(\bar{t}), \quad Y(\bar{t}) = 0, \tag{36}$$

where $\bar{t}$ denotes the time instant of the impact.

Now, introducing the basic change of state variable $Y = |X|$ the velocity condition in Eq. (36) becomes

$$\dot{Y} = \dot{X}\mathrm{sgn}(X), \tag{37}$$

and Eq. (35) yields

$$\ddot{X}(t) + 2\zeta\omega_0\dot{X}(t) + \omega_0^2 Y(t) = \mathrm{sgn}(X)W(t). \tag{38}$$

The ACF of the response process in Eq. (38) is known in closed form as

$$R_X(\tau) = \frac{q}{4\zeta\omega_0^3}\bar{R}_X(\tau) = \frac{q}{4\zeta\omega_0^3}e^{-\zeta\omega_0|\tau|}\left(\cos\omega_d\tau + \frac{\zeta\omega_0}{\omega_d}\sin\omega_d|\tau|\right), \tag{39}$$

where $\omega_d = \sqrt{\omega_0^2 - \zeta^2\omega_0^2}$. Thus, the ACF $R_Y(\tau)$ of the original response variable $Y(t)$ of the vibro-impact system is

$$R_Y(\tau) = \frac{q}{2\pi\zeta\omega_0^3}\left[\bar{R}(\tau)\arcsin\bar{R}(\tau) + \sqrt{1-\bar{R}^2(\tau)}\right], \tag{40}$$

when τ tends to infinity the ACF of $Y(\tau)$ approach to a limiting value $q/(2\zeta\omega_0^3) = \mu_Y^2$, being μ_Y the expectation value of $Y(t)$. The expression of ACF in Eq. (40) and the PSD of the zero-mean part of the response have been provided in [26]. In particular, such PSD, denoted as $S_{Y_0}(\omega)$, is obtained as Fourier transform of the ACF in Eq. (40) minus the value μ_Y^2. That is,

$$S_{Y_0}(\omega) = \frac{q}{\pi^2\zeta\omega_0^3}\int_0^\infty \left[\bar{R}(\tau)\arcsin\bar{R}(\tau) + \sqrt{1-\bar{R}^2(\tau)} - 1\right]\cos\omega\tau d\tau, \tag{41}$$

the integral in Eq. (41) can be evaluated in approximated form, or it can be used a certain number of CMs to obtain another characterization of the stochastic response of the vibro-impact problem at hand. In fact, both ACF and CF can be obtained with the direct evaluation of the CMs of the zero-mean part of process $Y(t)$, defined as

$$\hat{M}_{Y_0}(\gamma-1) = \frac{q}{2\pi\zeta\omega_0^3}\int_0^\infty \left[\bar{R}(\tau)\arcsin\bar{R}(\tau) + \sqrt{1-\bar{R}^2(\tau)} - 1\right]\tau^{\gamma-1}d\tau. \tag{42}$$

The knowledge of the complex quantities in Eq. (42) permits to obtain the ACF and the PSD by Eq. (9a) and (9b) respectively. The comparison between the exact ACF in Eq. (40) and the approximated one by CMs is depicted in Figure 7. With the aid of the same complex quantities the PSD is obtained and reported in Figure 8. In the latter case the depicted comparison is between the discrete Fourier transform of Eq. (41) (continuous line) and the CMs representation by Eq. (9b) (dotted line).

5. Concluding remarks

A new way to represent the CCF and CPSD by CMs and/or by CSMs has been pursued. It has been shown how to evaluate this complex entities starting from the knowledge of the CCF (CMs) or by the given CPSD (CSMs). These quantities are related to the Mellin transform and their knowledge permits to restore the CCF by the inverse Mellin transform. On the other hand, the inverse Mellin transform of the CSMs yields the CPSD. It has been shown that CMs and CSMs are related by a simple relation by using the properties of the Fourier transform. In other word, the CSMs are nothing else that the spectral counterparts of the CMs. It means that just the knowledge of one of the two kinds of moments permits to restore the other one and that allows to represent both CCF and CPSD. Therefore, both complex quantities have all information in time and in frequency domain.

The properties of the Mellin transform operator have been taken into account to demonstrate some important relationships of CMs and CSMs. In particular, a new representation of the CPSD and of the CCF

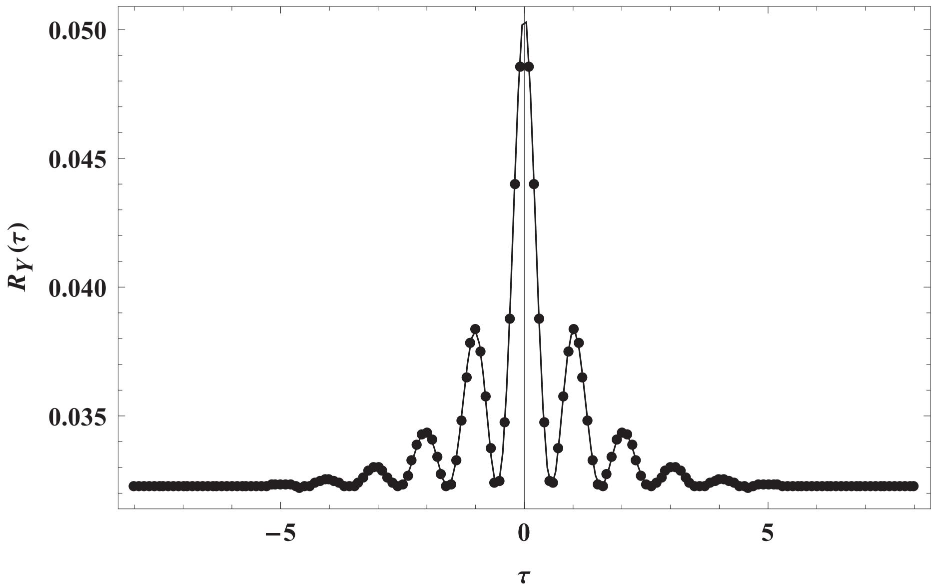

Figure 7: ACF obtained by Eq. (40) (continuous line) and by CMs (dotted line).

has been obtained as complex series expansion. This kind of series does not diverge, since the involved quantities have complex fractional order which real part is fixed and just imaginary part runs.

The capabilities of the proposed method have been shown considering three applications: i) the case of two linear oscillators forced by Gaussian white noise; ii) the characterization of the stochastic wind velocity field; iii) the characterization of the PSD and the ACF of a vibro impact system. From the examples the unbelievable accuracy of the method has been evidenced then it may be asserted that the CSMs are the third description of a Gaussian random process like CPSD and CCF.

AppendixA. Mellin transform and fundamental strip

Firstly the definition of the Mellin transform is reported

$$\mathrm{M}_f(\gamma-1) = \mathcal{M}\left\{f(\tau), \gamma\right\} = \int_0^{\infty} u(\tau)\tau^{\gamma-1}d\tau \tag{A.1}$$

$\mathrm{M}_f(\gamma-1)$ is a complex function in a complex variable γ, which existence is related to the fundamental strip (FS). The FS is a strip in the complex Mellin domain parallel to the imaginary axis, which bounds are two values of the real part ρ of γ. Then the condition for ρ to belong to the FS is generally written as

$$-p < \rho < -q \tag{A.2}$$

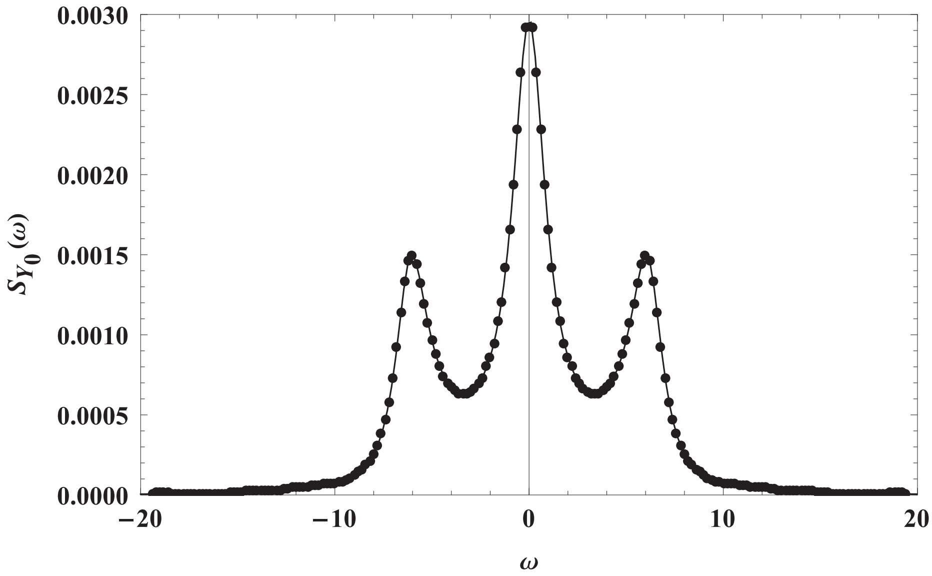

Figure 8: PSD obtained by discrete Fourier transform (continuous line) and by CMs (dotted line).

where p and q are strictly related to the asymptotic behavior of the function for $t \to 0$ and $t \to \infty$, respectively:

$$\begin{aligned} \lim_{t\to 0} f(t) &= \mathcal{O}(t^a) \quad \Rightarrow \quad -p = a \\ \lim_{t\to \infty} f(t) &= \mathcal{O}(t^b) \quad \Rightarrow \quad -q = b \end{aligned} \tag{A.3}$$

The function $f(\tau)$ can be constructed from the knowledge of $M_f(\gamma - 1)$ by the inverse Mellin transform operator:

$$f(\tau) = \frac{1}{2\pi}\int_{-\infty}^{\infty} M_f(\gamma-1)\tau^{-\gamma} d\eta \simeq \frac{\Delta\eta}{2\pi}\sum_{k=-m}^{m} M_f(\gamma_k - 1)\tau^{-\gamma_k}; \qquad \tau > 0 \tag{A.4}$$

The integral is performed along the imaginary axis η and the discretization in Eq. (A.4) is possible since $M_f(\gamma - 1) \to \pm 0$ for $\eta \to \pm\infty$.

Such an example is the FS of an exponential CF

$$R_x(\tau) = \sigma_x^2 \exp(-\alpha|\tau|) \tag{A.5}$$

where σ_x^2 and α are positive parameter. Since $\exp(-\alpha|\tau|)$ for $\tau = 0$ has a finite value the first bound of the FS is $-p = 0$, infact

$$\lim_{t\to 0} \exp(-\alpha|\tau|) = 1 = \mathcal{O}(t^0) \quad \Rightarrow \quad -p = 0 \tag{A.6}$$

For $t \to \infty$, $\exp(-\alpha|\tau|)$ behaves like $t^{-\infty}$, then we may write

$$\lim_{t\to 0} \exp(-\alpha|\tau|) = \mathcal{O}(t^{-\infty}) \quad \Rightarrow \quad -q = -\infty \tag{A.7}$$

Then the fundamental strip for this function is

$$0 < \rho < \infty \tag{A.8}$$

In the second case of the example in Sec. 4.2 we started from the knowledge of only the the CPSD $G_{V_1V_2}(\omega)$ and we can't obtain the analytical from of the cross-correlation. But CSMs of the CPSD are evaluated as CSMs of order $-\gamma$ and not with the Mellin transform operator (that gives CSMs of order $\gamma - 1$), then it has no sense to talk about FS. To overcome this problem we may pose, in integral of Eqs. (2), $-\gamma = \gamma^* - 1$: this allow to consider as Mellin trasform the integrals in Eqs. (2), then we may write CSMs Λ of the real and imaginary parts of the CPSD, reported in Eq. (15), as

$$\begin{aligned}\hat{\Lambda}_{V_1V_2}(\gamma^* - 1) &= \int_0^\infty \hat{G}_{V_1V_2}(\omega)\omega^{\gamma^*-1}d\omega \\ \tilde{\Lambda}_{V_1V_2}(\gamma^* - 1) &= \int_0^\infty \tilde{G}_{V_1V_2}(\omega)\omega^{\gamma^*-1}d\omega\end{aligned} \tag{A.9}$$

At this point we are able to do the same considerations made for the first example: for $\omega \to \infty$ both $\hat{G}_{V_1V_2}(\omega)$ and $\tilde{G}_{V_1V_2}(\omega)$ behave like $\omega^{-\infty}$, then in both cases $-\hat{q}, -\tilde{q} = -\infty$. At the origin $\hat{G}_{V_1V_2}(\omega)$ has a finite value, then $-\hat{p}^* = 0$, while $\tilde{G}_{V_1V_2}(\omega)$ is zero and near zero behaves like $-\omega^1$, then $-\tilde{p}^* = 1$. Summing up we may write:

$$\begin{aligned}0 < \hat{\rho}^* < \infty \\ -1 < \tilde{\rho}^* < \infty\end{aligned} \tag{A.10}$$

Finally, taking into account that $\rho^* - 1 = -\rho$, the value of ρ chosen must satisfy

$$\begin{aligned}-\infty < \hat{\rho} < 1 \\ -\infty < \tilde{\rho} < 2\end{aligned} \tag{A.11}$$

It obvious that since we have to use the same values for $\hat{\rho}$ and $\tilde{\rho}$, the choice of ρ must respect the more restrictive condition.
For the first case in Sec. 4.2 the restrictions on ρ are the same than for $\hat{G}_{V_1V_2}(\omega)$.

References

[1] Lin, Y. K., *Probabilistic Theory of Structural Dynamics*, Krieger Pub. (1976) 368 pages.

[2] Roberts, J. B., Spanos P. D., *Random Vibration and Statistical Linearization*, Dover Publications (2003) 446 pages.

[3] G. Cottone, M. Di Paola, A new representation of power spectral density and correlation function by means of fractional spectral moments, Prob. Eng. Mech. 25 (2010) 348-353.

[4] R. B. Paris, D. Kaminski, Asymptotics and Mellin-Barnes Integrals, Cambridge University Press, New York (2010).

[5] G. S. Samko, A. A. Kilbas, O. I. Marichev, Fractional integrals and derivatives: theory and applications, Gordon and Breach, New York (1993).

[6] I. Podlubny, Fractional Differential Equations, Academic Press, San Diego (1999).

[7] A. A. Kilbas, H. M. Srivastava, J. J. Trujillo, Theory and Applications of Fractional Differential Equations, Elsevier, Amsterdam (2006).

[8] E. Vanmarcke, Properties of spectral moments with applications to random vibrations, J. Eng. Mech. 98 (1972) 425-446.

[9] G. Cottone, M. Di Paola, On the use of fractional calculus for the probabilistic characterization of random variables, Prob. Eng. Mech. 24 (2009) 321-330.

[10] G. Cottone, M. Di Paola, R. Metzler, Fractional calculus approach to the statistical characterization of random variables and vectors, Physica A 389 (2010) 909-920.

[11] M. Di Paola, F. P. Pinnola, Riesz fractional integrals and complex fractional moments for the probabilistic characterization of random variables, Prob. Eng. Mech. 29 (2012) 149-156.

[12] G. Cottone, M. Di Paola, Fractional spectral moments for digital simulation of multivariate wind velocity fields, J. Wind Eng. Ind. Aerodyn. 99 (2011) 741-747.

[13] K. Runtemund, G. Cottone, G. M*ü*ller, Treatment of arbitrarily autocorrelated load functions in the scope of parameter identification, Computer and Structures 126 (2013) 29-40.

[14] M. Di Paola, Fokker-Planck equation solved in terms of complex fractional moments, Prob. Eng. Mech. 38 (2014) 70-76.

[15] G. Alotta, M. Di Paola, Probabilistic characterization of nonlinear systems under α-stable white noise via complex fractional moments, Physica A: Stat. Mech. Appl. 420 (2015) 265-276.

[16] A. Di Matteo, M. Di Paola, A. Pirrotta, Probabilistic characterization of nonlinear systems under Poisson white noise via complex fractional moments, Nonlinear Dyn. 77 (2014) 729-738.

[17] F. P. Pinnola, Statistical correlation of fractional oscillator response by complex spectral moments and state variable expansion, Commun. Nonlinear Sci. Numer. Simulat. 39 (2016) 343-359.

[18] G. Alotta, M. Di Paola, G. Failla, A Mellin transform approach to wavelet analysis, Commun. Nonlinear. Sci. Numer. Simulat. 28 (2015) 175-193.

[19] M. Shinozuka, C. B. Yun, H. Seya, Stochastic methods in wind engineering, J. Wind Eng. Ind. Aerodyn. 36 (1990) 829-843.

[20] M. Di Paola, Digital simulation of wind field velocity, J. Wind Eng. Indust. Aerodyn. 74-76 (1998) 91-109.

[21] G. Solari, Gust buffeting. I: peak wind velocity and equivalent pressure, J. Struct. Eng. 119 (1993) 365-382.

[22] L. Carassale, G. Piccardo, G. Solari, Double modal transformation and wind engineering applications, J. Eng. Mech. ASCE 127 (5) (2001) 432-439.

[23] Y. Zhou, T. Kijewski, A. Kareem, Aerodynamic loads on tall buildings: an interactive database, J. Struct. Eng. 129 (2003) 394-404.

[24] L. Carassale, G. Solari, Monte Carlo simulation of wind velocity fields on complex structures, J. Wind Eng. Ind. Aerodyn. 94 (2006) 323-339.

[25] A. Kareem, Numerical simulation of wind effects: a probabilistic perspective, J. Wind Eng. Indust. Aerodyn. 96 (2008) 1472-1497.

[26] M. Dimentberg, Z. Hou, M. Noori, Spectral density of a non-linear single-degree-of-freedom system's response to a white-noise random excitation: a unique case of an exact solution, Int. J. Non-Linear Mech. 30 (1995) 673-676.

[27] M. Di Paola, C. Bucher, Ideal and physical barrier problems for non-linear systems driven by normal and Poissonian white noise via path integral method, Int. J. Non-Linear Mech. 81 (2016) 274-282.